Mehran University Research Journal of Engineering and Technology

https://doi.org/10.22581/muet1982.2303.13

2023, 42(3) 119-128

Modeling and estimation of solar radiation of Karachi through artificial neural network (ANN) using temperature and dew-point

Atif Idrees [a, d], Naeem Sadiq [b], Mahwish M Khan [c, *], Syed A Hassan [d], Zaheer Uddin [e]

[a] *Department of Basic Sciences, DHA Suffa University, Karachi, Pakistan*

[b] *Institute of Space Science and Technology, University of Karachi, Karachi, Pakistan,*

[c] *Department of Applied Chemistry and Chemical Technology, University of Karachi, Karachi, Pakistan*

[d] *Department of Mathematics, University of Karachi, Karachi, Pakistan*

[e] *Department of Physics, University of Karachi, Karachi, Pakistan*

* Corresponding author, Mahwish M Khan, E-mail: mmobeen@uok.edu.pk

Received: 09 March 2023, Accepted: 26 June 2023, Published: 01 July 2023

K E Y W O R D S

Artificial Neural Network

Global Radiation

Diffused Radiation

Direct Beam Solar Radiation

Temperature

Dew-point

A B S T R A C T

The most influential source of energy in our lives is solar energy. Solar energy reaches the earth in three different forms, i.e., Global, diffused, and Direct Solar Radiation. The Solar flux at the earth's surface depends on the intensity of these radiations and is a function of the values of latitude and longitude. The earth's temperature and hence dewpoint are greatly affected by solar flux. This idea is used for predicting solar radiation with input parameters, temperature, and dewpoint along with day number and month. The method of prediction of solar radiation used in the study is Artificial Neural Network (ANN). ANN has four variables in the input, ten neurons in the hidden layer, and three output parameters GSR. DSR and BSR. Six different types of errors, namely, Root Mean Square error (RMSE), Mean Absolute Error (MABE), Mean percent error (MAPE), Chi-square, Coefficient of Determination, Kolmogorov Smirnov, have been calculated for training, testing, and validation mode to check the accuracy of estimation. The values of all the errors are low, which indicates the prediction of solar radiation is reliable.

1. Introduction

Solar Radiation has a socio-economic impact on our daily lives, in addition to the various industries, such as photovoltaic, manufacturing, farming, architectural design, etc. Therefore, its forecasting has great importance to scientists and users for research and routine tasks. To predict solar radiation, researchers created some strategies. Qiu *et al*. proposed the XGboost model, which combines temperature and geographical data to estimate the daily radiations for those areas where historical data is not accessible [1]. Using a Long short-term memory (LSTM) network and gated recurrent unit (GRU) network, Singla *et al*. developed two deep learning models for forecasting solar irradiance globally; these deep learning networks are trained using the climatic variables dew point, pressure, temperature, solar zenith angle, relative humidity, wind speed, and precipitation. The experiment outcomes demonstrated the effectiveness of GRU and LSTM networks [2]. Gouda *et al*. found in their study that the temperature and dew point enhance the performance of the models in humid environments [3]. Through Levenberg-Marquardt, Bayesian Regularization, and Scaled Conjugate Gradient in the research paper in all three instances, Choudhary *et al.* found that the network's overall performance is quite good for prediction of solar

radiation [4]. Li *et al*. compared different models and suggested that the model on temperature, precipitation, and dew point performed better in spring [5]. The solar radiation data can also be utilized to calculate the solar energy potential at Damak. According to Shrestha *et al*., the dew point is highly connected with air temperature as opposed to relative humidity, as revealed by the correlation matrix [6]. Among several methods, Munir A. *et al*. conclude that Artificial Neural Network (ANN) is a very useful tool for solar radiation forecast accuracy. Their analysis revealed that temperature and dew point parameters are the most suitable and accurate for predicting solar radiation [7]. In diverse climates in 2020 and 2050, Akhlaghi *et al*. developed a Deep Neural Network (DNN) model for a Guideless Irregular Dew Point Cooler (GIDPC) that is understandable and interpretable. [8]. Qazi *et al*. concluded that the neural networks and adaptive neuro-fuzzy inference systems improve prediction accuracy for hourly and monthly solar radiation estimates, respectively. It is determined that more study on ANN and its applications is necessary. The employment of ANN in the industry may be aided by the encouraging outcomes that have been produced [9]. To forecast worldwide solar radiation on a horizontal surface at various locations, the temperature-based models fit well. The findings of Hassan *et al*. demonstrate the importance and applicability of the novel temperature-based models for the quick and precise estimation of the monthly average daily global solar radiation on a horizontal surface [10]. Ekici, C., and Teke, I. tried to make total global solar radiation modeled through parameters like dew point temperature, visibility, and maximum and minimum air temperatures are used and accurate results were obtained [11]. Dong *et al*. concluded that the most fundamental meteorological variables were temperature and humidity, and adding unnecessary additional variables impacted the model's ability to make predictions. At hourly scales, the component Month would be more significant than the factor Time [12]. Ukhurebor discovered the linear relationship between the air temperature and dew point, *et al*., the air temperature has a considerable impact on the dew point temperature, and a rise in the air temperature would also cause an increase in the dew point temperature [13]. The study by Sein *et al*. concluded that the winter saw the strongest positive seasonal correlation between daily mean air temperature and dew point temperature. In contrast, the rainy season saw the lowest correlation [14].

2. Material and methods

2.1 Artificial Neural Network

Neural networks have been successfully employed in various fields of science and technology for the last two decades and have been more useful than traditional statistical tools. Among all the fields, ANN is widely used in atmospheric science, environmental chemistry, and climatology to predict short and long-term changes with time for locations with known or unknown meteorological data.

The architecture of the neural network model is based on multiple node layers interconnected with neurons. Each neuron has its activation function provided with individual weight and biases. These layers must include input layers, hidden layers, and output layers. The input layer is fed with the data set, which is further divided into training, testing, and validation data sets. Hidden layers perform calculations, while the output layer is responsible for model generation.

ANN architecture has been built to predict three types of solar radiations in Karachi (fig. 1). The input layer has dew point, temperature, and the number of days as variables, and each is connected to the neurons in the hidden layer through some weights and a bias. The Levenberg-Marquardt algorithm (LMA) fits non-linear least square data curves. The training data set is treated by LMA under the input layer of the ANN domain. Once the Proposed model is tested against the meteorological data, it is used to predict input values after validation.

These weights are known as the gradient or coefficient of the variable. The neuron receives data using the following equation

$$y_{hidden} = \sum_{i=1}^{n} w_i y_i + b_{input} \quad (1)$$

Here y_i are the n, variables and w_i are the n weight and b_{input} is the input bias. A non-linear transformation through an activation function is applied to the eq. (1) for final information at neurons. One of the activation functions is a sigmoidal function; we used this function in the proposed ANN model.

$$f(y_{hidden}) = \frac{1}{1+e^{-y_{hidden}}} \quad (2)$$

The hidden layer is connected to the output layer and the neuron transfer information to the output layer. The output data is compared with the known data, and the error is calculated; if the error does not meet the convergence criterion, the process is repeated using backpropagation. In backpropagation, new weights are calculated till one gets optimal weights, which minimize the difference between ANN output and actual values.

2.2 Estimation of solar radiations

Accurate estimation of solar energy is a difficult task by conventional statistical methods. ANNs offer various architectures to solve this problem, and promising results are obtained. These architectures may use minimum variables as input data. This paper uses the number of Days, Months, and Dew points and temperatures to find the three types of solar radiation. ANN model is developed to estimate Diffused solar radiations (DSR), global solar radiations (GSR), and direct beam radiations (DBR) for Karachi city. This model is built with one hidden layer with ten neurons. The performance of the network was the best for ten neurons.

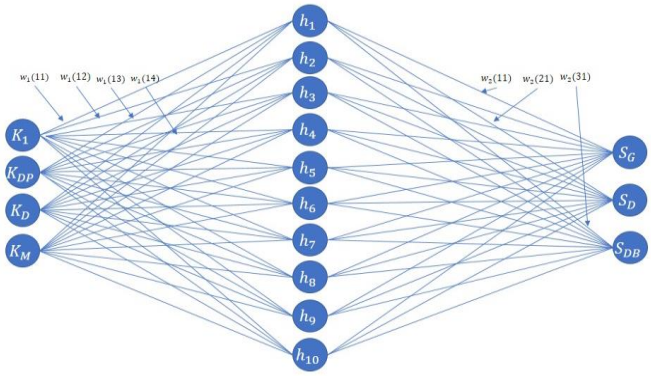

Fig. 1. ANN network for the estimation of Solar Radiation, In input K_1, K_{DP}, K_D, and K_M represent temperature, Dew point, Day, and month respectively. In output S_G, S_D, and S_D are Global, Direct Beam and Diffused solar radiation

2.3 Data

Data of temperature and dew point for three years {i.e., 2016, 2018 and 2019 (The data for 2017 was incomplete)} were used in this study and were provided by Pakistan Meteorological Department. Three types of Solar (i.e., DSR, GSR, and DBR) have been estimated for these two meteorological parameters.

3. Results and Discussion

Every ANN network has three components, input, hidden layer(s), and output. The input part in this ANN network consists of four variables, day, month, temperature, and dew point. The reason for taking the earth's temperature and dew point as the input parameter is their close link to solar radiations. A single hidden layer is used, which consists of 10 neurons. Three different solar radiation were estimated as the output of the network. Sixty percent of input data was used for training the network; the remaining 40 percent was used to test the trained network. Fifty percent random data was used for validation purposes. The residues have been calculated by taking the absolute difference between estimated and recorded values of solar radiations. Three years (2016, 2018, 2019) of daily solar radiation data was used in the study. The data for 2017 was incomplete. Three types of solar Radiation, GSR, DSR, and BSR, were estimated and compared for these three years. Fig. 1-3 show daily global radiation, fig. 4-6 show daily direct beam solar radiation and fig. 7-9 show daily diffused solar radiations for 2016, 2018, and 2019. Each figure has three parts (a,b,c), training mode, testing mode, and validation mode, along with corresponding residues. It can be seen that the values of residues are sufficiently small, which is characteristic of a good ANN network.

For 2016 training data, the absolute difference regarding DSR, DBR, and GSR comes out as less than $4x10^{-2}$ %, $4x10^{-1}$ %, and $7x10^{-2}$ %, respectively. Regarding 2018, the same values are less than 5 x 10^{-2} %, 4 x 10^{-1}%, and 8 x 10^{-2}%, respectively, while for 2019, the absolute difference comes out to less than 6 x 10^{-2} %, 4.5 x 10^{-1} %, and 8 x 10^{-2}%, respectively. Similarly, these values are also estimated for the testing and validation for the above years (fig 1-9).

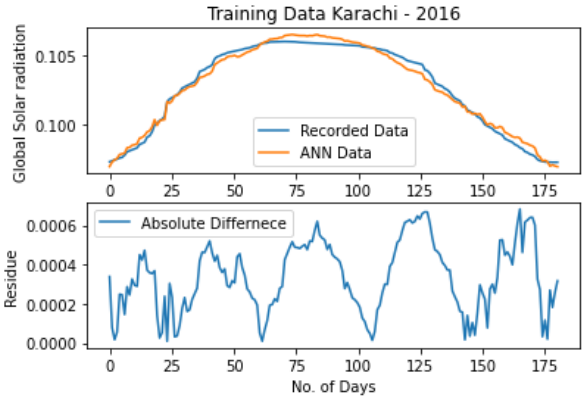

Fig. 2 (a)

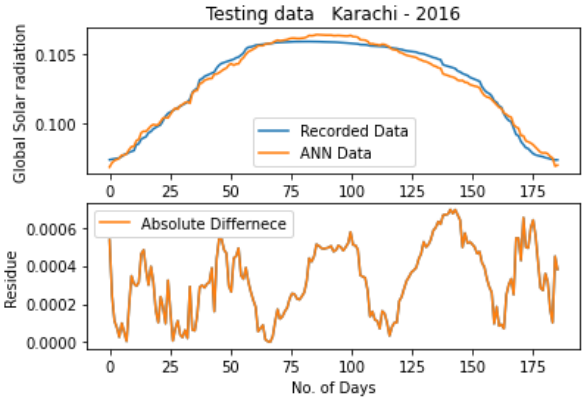

Fig.2 (b)

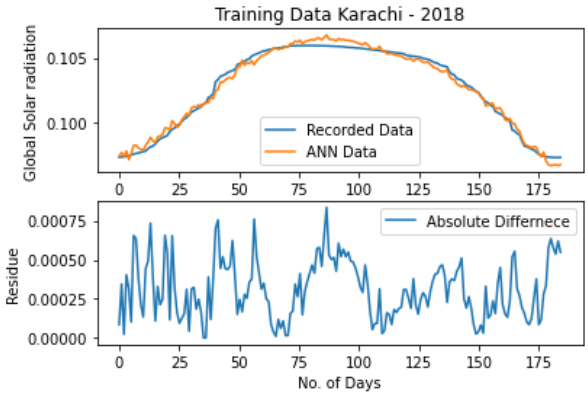

Fig. 2 (c)

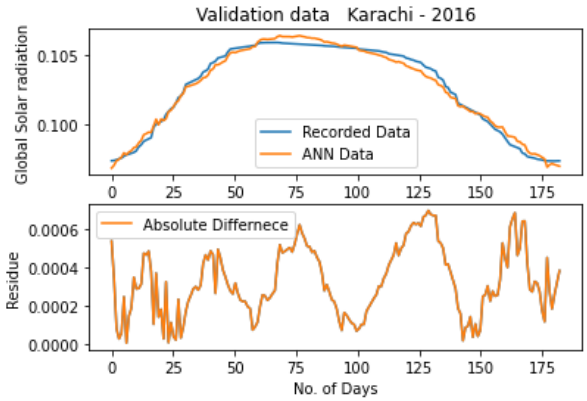

Fig. 3 (a)

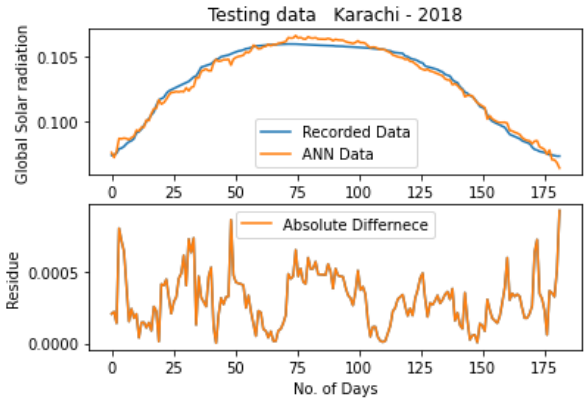

Fig. 3 (b)

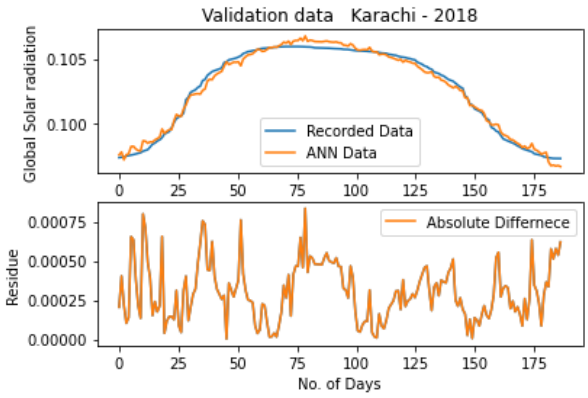

Fig. 3 (c)

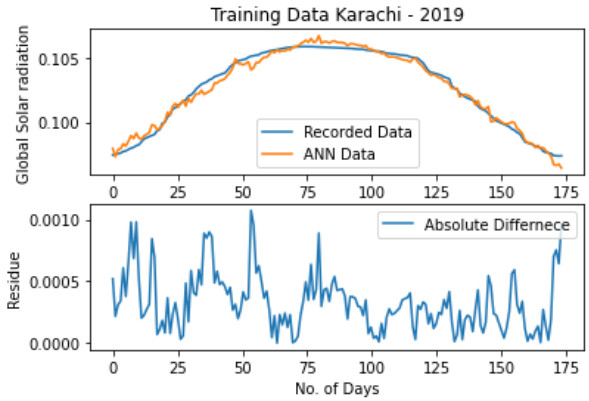

Fig. 4 (a)

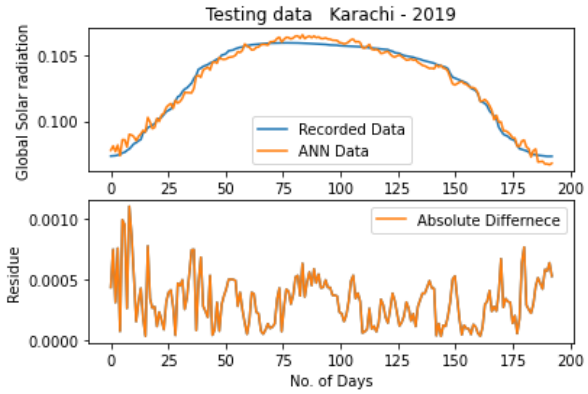

Fig. 4 (b)

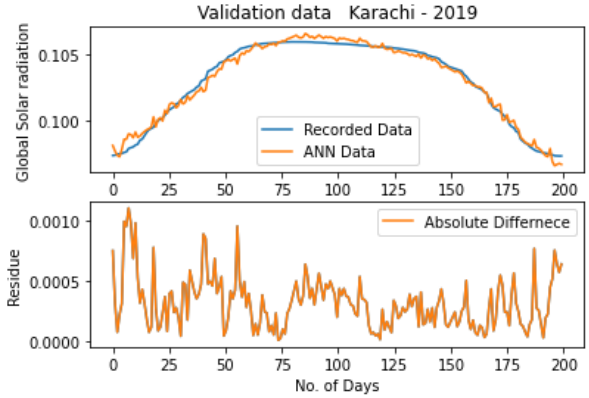

Fig. 4 (c)

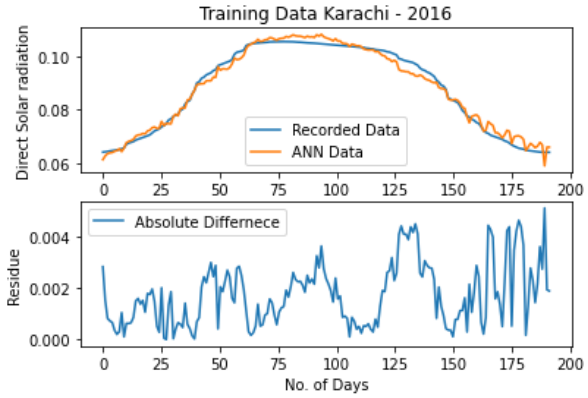

Fig. 5 (a)

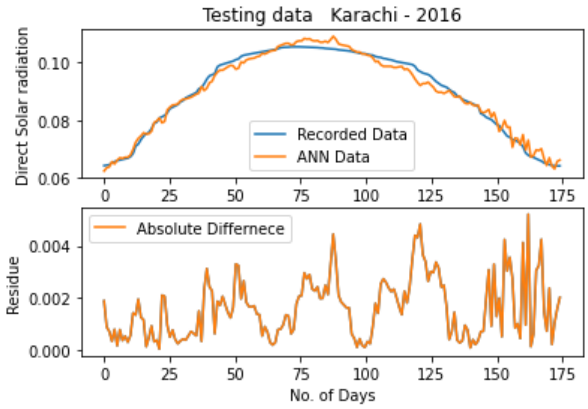

Fig. 5 (b)

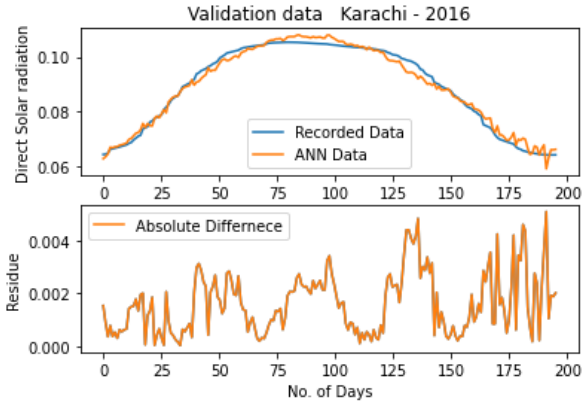

Fig. 5 (c)

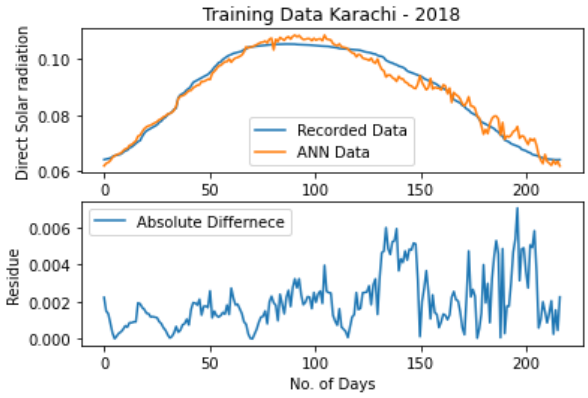

Fig. 6 (a)

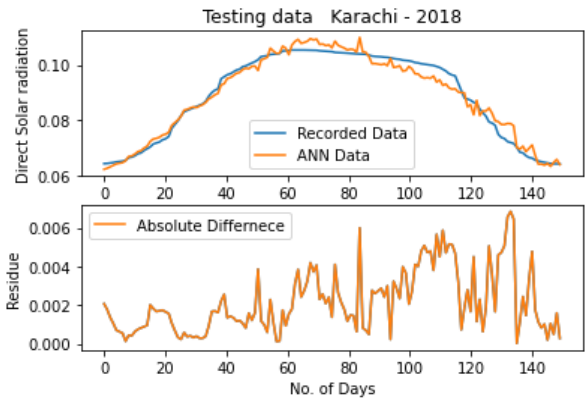

Fig.6 (b)

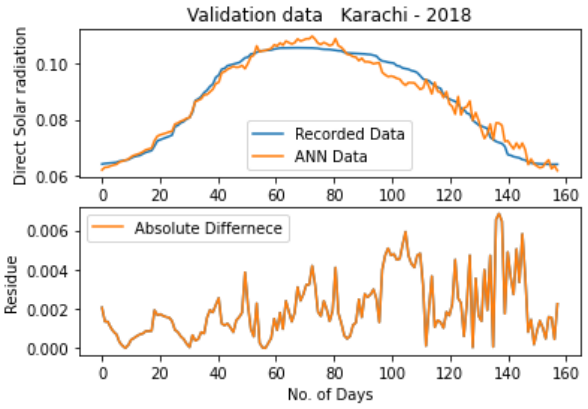

Fig. 6 (c)

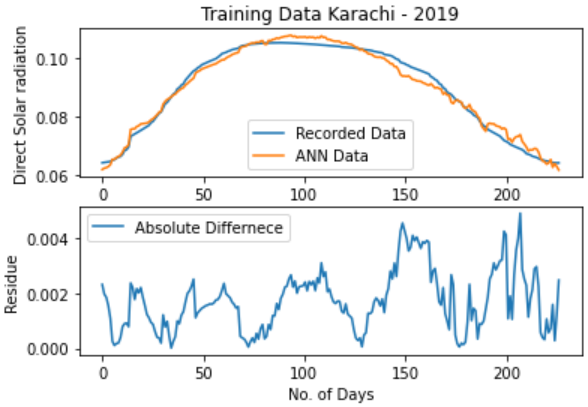

Fig. 7 (a)

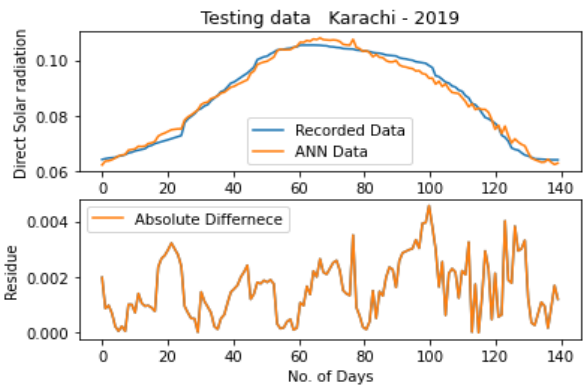

Fig. 7 (b)

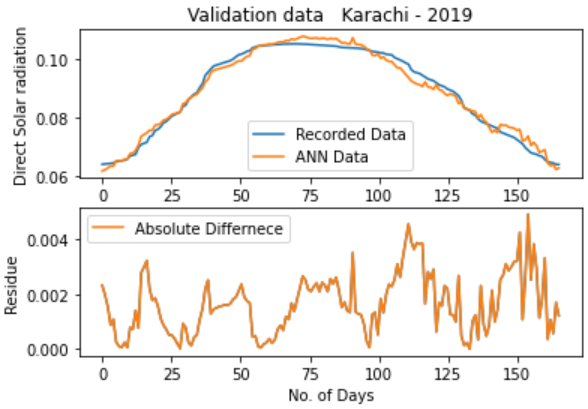

Fig.7 (c)

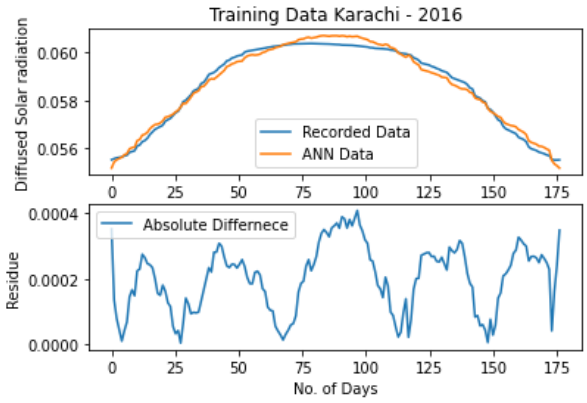

Fig. 8 (a)

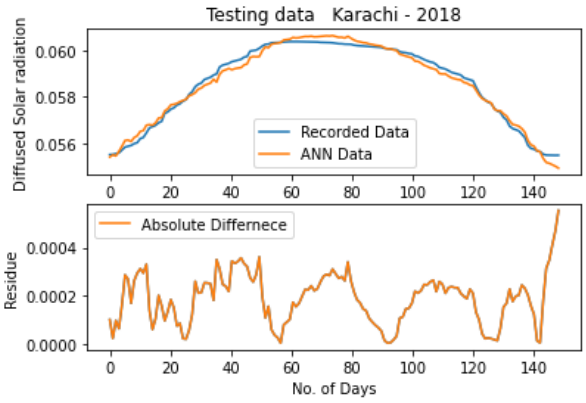

Fig. 8 (b)

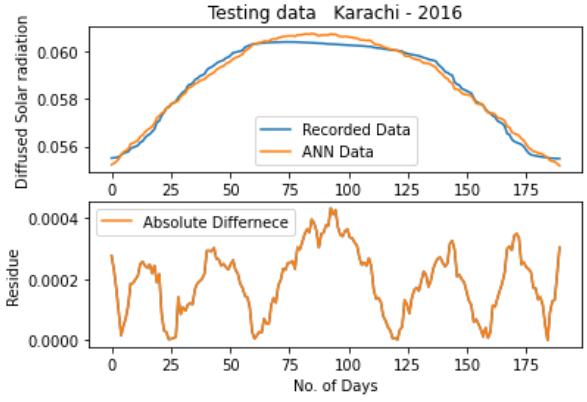

Fig. 8 (b)

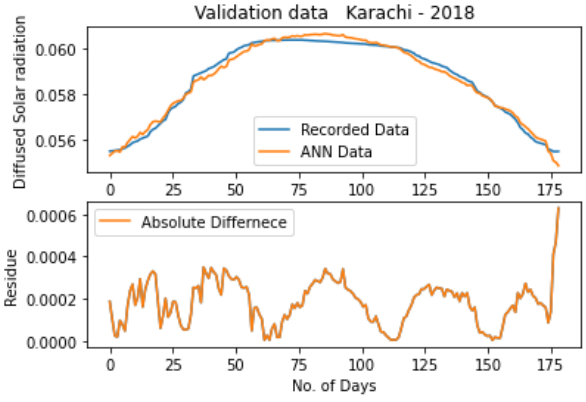

Fig. 9 (c)

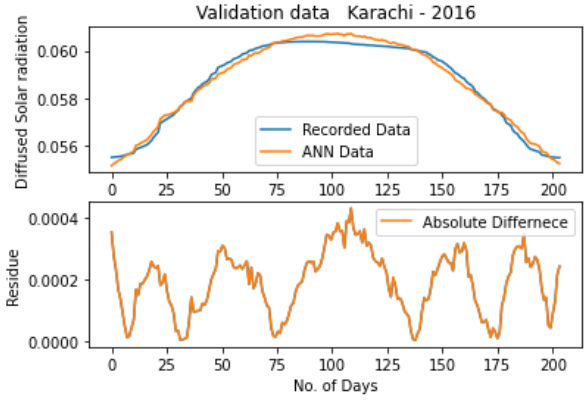

Fig. 8 (c)

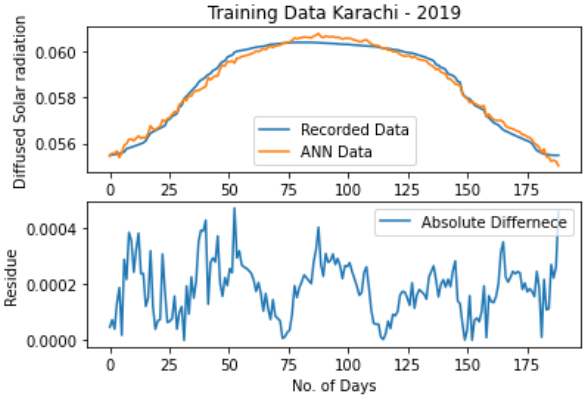

Fig. 10 (a)

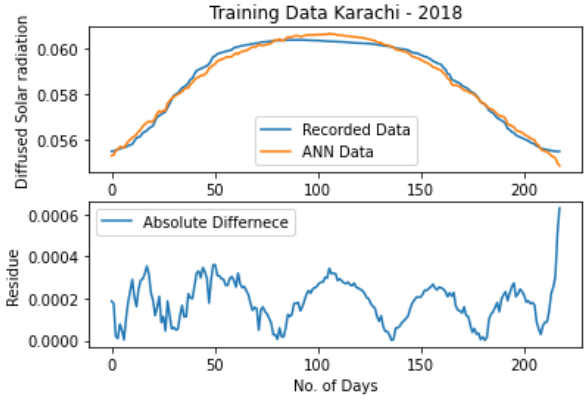

Fig. 9 (a)

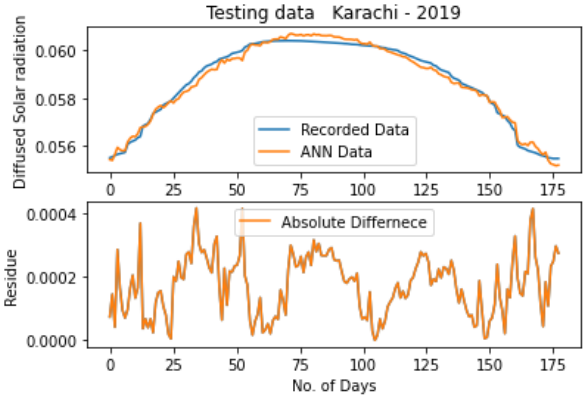

Fig. 10 (b)

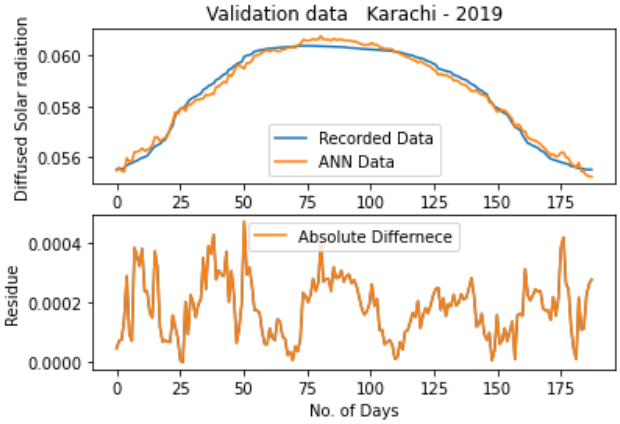

Fig. 10 (c)

Tables 1-3 show the weights of the ANN model for GSR, DSR, and BSR. Each table has three sub-tables for the years 2016, 2018, and 2019. For each year, there are five columns; the first four columns give weights that link input values and neurons in the hidden layer, and the fifth column gives weight that connects neurons in the hidden layer with the output variables.

Table 1

Weights for Global Solar Radiation Estimation

	w11	0.2823	-0.1547	-0.6902	-1.6030	0.1988	-1.2109	-1.3258	-0.7818	0.2070	-0.6114
	w12	-0.0579	-0.1239	-0.0341	-0.2216	-0.3161	-0.5684	-0.9741	-0.8286	-0.5827	-0.0373
2016	w13	2.1176	0.9566	-1.5446	-6.8705	2.0267	-7.5236	-7.4409	-9.5460	2.1185	-9.3204
	w14	0.3561	-0.4425	-0.3440	-0.4563	-0.1082	-0.5619	-0.8646	-0.5917	0.5638	0.2423
	w2	-0.8590	-0.5856	-0.5280	0.0191	-0.7278	-0.0104	-0.0628	-0.4007	-0.8473	-0.4800
	w11	-0.5904	-1.4241	-0.4623	-1.1216	-0.2602	-0.2479	-1.1549	-0.1191	-1.2666	-0.1968
	w12	-0.4198	-0.4414	-0.3650	-0.4611	-0.2403	-0.6932	-0.6791	-0.6927	0.0683	-0.5123
2018	w13	1.7169	-8.8939	0.1592	-8.4572	1.2088	1.8658	-5.7973	1.9877	-7.6060	0.8200
	w14	-0.5261	-0.3100	-0.5493	0.0236	0.2494	0.3022	-0.6439	0.4023	-0.3867	0.2011
	w2	-0.5887	-0.3722	-0.4644	-0.4198	-0.5495	-0.6400	-0.0153	-0.7752	-0.1716	-0.5035
	w11	-0.3355	-0.8692	-1.1354	-1.1853	-0.8564	-1.0458	-0.1747	-0.7852	-0.8156	-0.3413
	w12	-1.0577	-0.8538	-0.0499	-0.4225	-0.4040	-0.7748	-0.4587	0.1388	-0.3880	-0.6971
2019	w13	1.8914	-8.7174	-5.7335	1.8039	-7.9112	-7.2723	0.3952	-5.5529	1.6624	1.3935
	w14	0.2298	0.3059	0.2852	-0.2650	-0.3371	-0.3727	-0.3643	0.3045	-0.0276	0.2451
	w2	-0.7993	-0.4074	-0.1287	-0.7173	-0.2713	-0.2151	-0.5648	-0.0257	-0.7085	-0.6685

Table 2

Weights for Diffused Solar Radiation Estimation

	w11	1.064	-0.690	0.713	-0.245	-1.776	-1.277	-0.843	-1.166	0.009	0.491
	w12	0.259	-0.426	0.129	0.049	-0.538	-0.411	-0.374	-0.683	-0.517	0.197
2016	w13	2.957	-7.972	3.244	-2.426	-9.159	-7.894	-7.231	-9.540	0.653	2.417
	w14	0.473	-0.114	0.238	-0.556	-0.383	-0.002	0.136	-0.229	-0.419	0.038
	w2	-0.963	-0.352	-1.037	-0.653	-0.155	-0.358	-0.409	-0.112	-0.759	-0.879
	w11	-0.033	-1.188	-0.235	-0.430	-0.332	-1.806	-2.028	-2.345	0.932	-0.123
	w12	-0.118	-0.722	-0.196	-0.789	0.069	-0.665	-0.810	-0.766	0.732	-0.626
2018	w13	1.787	-6.911	1.355	-6.563	1.911	-8.921	-9.031	-8.700	2.466	0.652
	w14	-0.457	-0.526	0.239	-0.074	-0.144	-0.421	-0.505	-0.120	0.552	0.062
	w2	-0.819	-0.658	-0.766	-0.632	-0.865	-0.051	-0.053	-0.101	-1.025	-0.728
	w11	-0.701	0.249	-0.880	-0.658	-0.567	0.167	-1.208	0.047	-1.017	-0.449
2019	w12	-0.244	-0.430	-0.777	0.064	-0.492	0.001	-0.319	-0.730	-0.554	-0.215
	w13	-8.956	1.798	-7.869	1.898	-2.808	1.811	-6.552	1.783	-6.111	-0.302

Table 3

Weights for Direct Beam Solar Radiation Estimation

	w11	1.635	-1.470	5.510	5.504	-1.831	-3.595	-4.410	-4.517	-1.799	3.965
	w12	2.927	-1.641	7.399	6.636	-1.522	-7.499	-8.977	-9.115	-4.958	6.695
2016	w13	-13.314	-3.258	-12.746	-12.805	-3.250	3.483	3.521	3.522	3.435	-12.919
	w14	-0.157	-0.908	1.366	1.604	-0.608	-0.443	-0.749	-0.664	-0.622	1.126
	w2	-0.493	0.781	-0.952	-0.902	0.969	-1.028	-1.188	-1.182	-0.655	-0.835
	w11	-10.108	4.613	1.207	-4.107	-7.658	2.330	-7.297	13.327	1.794	11.774
	w12	-14.849	8.700	2.368	-6.430	-10.534	3.679	-10.455	19.112	3.098	17.056
2018	w13	4.812	-18.563	-12.448	4.190	4.538	-15.872	4.504	-15.906	-14.845	-16.515
	w14	0.640	-0.250	0.961	0.360	0.561	0.744	0.915	-0.271	0.537	-0.216
	w2	-1.108	-0.433	0.167	-0.489	-0.852	-0.051	-0.888	-0.964	0.026	-0.879
	w11	0.216	2.464	-3.997	-0.362	-2.679	0.975	-4.283	-1.736	1.683	-4.502
	w12	3.398	7.208	-8.304	2.188	-5.433	4.921	-9.007	-0.909	6.607	-7.055
2019	w13	-13.163	-13.468	3.370	-13.145	3.413	-13.471	3.386	-3.524	-13.475	3.428
	w14	0.102	1.807	-0.370	1.091	-0.602	1.139	-1.229	-0.896	1.616	-0.821
	w2	-0.362	-0.761	-1.038	-0.415	-0.748	-0.529	-1.065	0.972	-0.749	-0.966

The goodness of estimation of solar Radiation by ANN can be measured by comparison of estimated values with the recorded value. Various criteria compare estimated and measured values. Six such criteria, namely, Root Mean Square Error (RMSE), Mean Absolute Error (MABE), Mean Absolute Percent Error (MAPE), Chi-square statistic, coefficient of determination, and Kolmogorov Smirnov test, were used for the comparison of the goodness of estimated values (Table 4-6). The maximum value of RMSE was seen in global solar Radiation of 2016, which was 0.73% in testing mode. The maximum value of MABE occurred for 2018, which was 0.22% in validation mode. The maximum value of MAPE also occurred in 2018, which was 0.0243% in direct mode. The maximum value of Chi comes out as 0.01% in the testing mode of 2016. The minimum value of R-square is 0.9000% for testing 2016 global. The maximum value of Kolmo-S is 0.71% in the Testing mode of 2018.

Table 4

Global Solar Radiation

	2016			2018			2019		
	Training	Testing	Validation	Training	Testing	Validation	Training	Testing	Validation
RMSE	0.0004	0.0011	0.0004	0.0006	0.0004	0.0004	0.0004	0.0004	0.0004
MABE	0.0003	0.0009	0.0004	0.0005	0.0003	0.0003	0.0003	0.0003	0.0003
MAPE	0.0033	0.0134	0.0034	0.0046	0.0030	0.0030	0.0033	0.0031	0.0030
Chi	0.0000	0.0000	0.0000	0.0000	0.0000	0.0000	0.0000	0.0000	0.0000
R-Square	0.9827	0.9	0.9791	0.9642	0.9852	0.9876	0.9823	0.9839	0.9841
Kolmo-S	0.0007	0.00251	0.0010	0.0015	0.0009	0.0008	0.0011	0.0011	0.0010

Table 5

Diffused Solar Radiation

	2016			2018			2019		
	Training	Testing	Validation	Training	Testing	Validation	Training	Testing	Validation
RMSE	0.0002	0.0002	0.0002	0.0002	0.0002	0.0002	0.0002	0.0002	0.0002
MABE	0.0002	0.0002	0.0002	0.0002	0.0002	0.0002	0.0002	0.0002	0.0002
MAPE	0.0034	0.0033	0.0032	0.0031	0.0032	0.0031	0.0031	0.0030	0.0031
Chi	0.0000	0.0000	0.0000	0.0000	0.0000	0.0000	0.0000	0.0000	0.0000
R-Square	0.9824	0.9842	0.9849	0.9856	0.9837	0.9848	0.9863	0.9857	0.9860
Kolmo-S	0.0004	0.0004	0.0004	0.0006	0.0006	0.0006	0.0005	0.0004	0.0005

Table 6

Direct Beam Solar Radiation

	2016			2018			2019		
	Training	Testing	Validation	Training	Testing	Validation	Training	Testing	Validation
RMSE	0.0021	0.0020	0.0020	0.0025	0.0027	0.0026	0.0019	0.0018	0.0017
MABE	0.0017	0.0016	0.0016	0.0020	0.0022	0.0021	0.0015	0.0014	0.0014
MAPE	0.0204	0.0180	0.0186	0.0234	0.0243	0.0238	0.0172	0.0165	0.0158
Chi	0.0001	0.0000	0.0000	0.0001	0.0001	0.0001	0.0000	0.0000	0.0000
R-Square	0.9814	0.9803	0.9825	0.9709	0.9684	0.9722	0.9843	0.9859	0.9862
Kolmo-S	0.0051	0.0052	0.0051	0.0071	0.0069	0.0069	0.0058	0.0048	0.0049

4. Conclusion

Four-inputs ANN network has been developed and implemented to estimate three types of solar radiation. Three years of solar radiation data for 2016, 2018, and 2019 were used to carry out this research. Daily solar radiations were used for training testing and validation purpose. The ANN has a single hidden layer with ten neurons that get information from four input parameters, i.e., day of the month, the month of the year, temperature, and dewpoint. Three types of radiations (GSR, DBR, and DSR) are obtained as an output from the neurons in the hidden layer. For every year and every type of solar radiation, three types of plots with residuals were generated according to training testing and validation. There are 27 such plots; in each case, the correlation coefficient was 0.99. Six criteria were used to check the reliability of ANN estimation: Root Mean Square Error RMSE, Mean Absolute Error MABE, Mean percent error MAPE, Chi-square, Coefficient of Determination, Kolmogorov Smirnov. These errors are given in tables 1-3. The lower values of errors support the goodness of network estimation. The Kolmogorov-Smirnov criteria, which shows the largest difference between estimated and recorded solar radiation values, also have a low value.

5. References

[1] R. Qiu, C. Liu, N. Cui, Y. Gao, L. Li, Z. Wu and M. Hu, “Generalized extreme gradient boosting model for predicting daily global solar radiation for locations without historical data”, Energy Conversion and Management, 258, 115488, 2022.

[2] P. Singla, M. Duhan, and S. Saroha, "One hour ahead solar irradiation forecast by deep learning network using meteorological variables”, Control and Measurement Applications for Smart Grid" Springer, Singapore, pp. 103-113, 2022.

[3] S. G. Gouda, Z. Hussein, S. Luo, P. Wang, H. Cao, and Q. Yuan, “Empirical models for estimating global solar Radiation in Wuhan City, China”, The European Physical Journal Plus, 133(12), 1-10, 2018.

[4] A. Choudhary, D. Pandey, and S. Bhardwaj, “Artificial neural networks based solar radiation estimation using back propagation algorithm”, International Journal of Renewable Energy Research, 10(4), 1566-1575, 2020.

[5] M. F. Li, H. B. Liu, P. T. Guo, and W. Wu, “Estimation of daily solar Radiation from routinely observed meteorological data in Chongqing, China”, Energy Conversion and Management, 51(12), 2575-2579, 2010.

[6] A. K. Shrestha, A. Thapa, and H. Gautam, “Solar radiation, air temperature, relative humidity, and dew point study: Damak, jhapa, Nepal”, International Journal of Photoenergy, 2019.

[7] A. Munir, A. Khattak, K. Imran, A. Ulasyar, A. U. Haq, A. Khan, and N. Ullah, “Artificial neural network based simplified one day ahead forecasting of solar photovoltaic power generation”, Journal of Engineering Research, 10(1A), 175-189, 2022.

[8] Y. G. Akhlaghi, K. Aslansefat, X. Zhao, S. Sadati, A. Badiei, X. Xiao, and X. Ma, “Hourly performance forecast of a dew point cooler using explainable artificial intelligence and evolutionary optimisations by 2050”, Applied Energy, 2021, 281, 116062.

[9] A. Qazi, H. Fayaz, A. Wadi, R. G. Raj, N. A. Rahim, and W. A. Khan, “The artificial neural network for solar radiation prediction and designing solar systems: a systematic literature review”, Journal of cleaner production, 2015, 104, 1-12.

[10] G. E. Hassan, M. E. Youssef, Z. E. Mohamed, M. A. Ali, and A. A. Hanafy, “New temperature-based models for predicting

global solar radiation", Applied energy, 179, 437-450, 2016.

[11] C. Ekici, and I. Teke, "Global solar radiation estimation from measurements of visibility and air temperature extremes", Energy Sources, Part A: Recovery, Utilization, and Environmental Effects, 41(11), 1344-1359, 2019.

[12] J. Dong, W. Zeng, G. Lei, L. Wu, H. Chen, J. Wu, and A. K. Srivastava, "Simulation of dew point temperature in different time scales based on grasshopper algorithm optimized extreme gradient boosting", Journal of Hydrology, 606, 127452, 2022.

[13] K. E. Ukhurebor, T. B. Batubo, I. C. Abiodun, and E. Enoyoze, "The influence of air temperature on the dew point temperature in Benin City, Nigeria", Journal of Applied Sciences and Environmental Management, 21(4), 657-660, 2017.

[14] Z. M. Sein, I. Ullah, V. Iyakaremye, K. Azam, X. Ma, S. Syed, and X. Zhi, "Observed spatiotemporal changes in air temperature, dew point temperature and relative humidity over Myanmar during 2001–2019", Meteorology and Atmospheric Physics, 134(1), 1-17, 2022.

